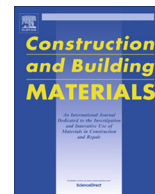




Contents lists available at ScienceDirect

Construction and Building Materials

journal homepage: www.elsevier.com/locate/conbuildmat

Effect of high temperature on the mechanical properties of basalt fibre self-compacting concrete as an overlay material

James H. Haido ^{a,*}, Bassam A. Tayeh ^b, Samadar S. Majeed ^{c,d}, Mehmet Karpuzcu ^d^a Department of Civil Engineering, College of Engineering, University of Duhok, Kurdistan Region, Iraq^b Civil Engineering Department, Faculty of Engineering, Islamic University of Gaza^c College of Engineering, Nawroz University, Kurdistan Region, Iraq^d Civil Engineering Department, Faculty of Engineering, Hasan Kalyoncu University, Turkey

HIGHLIGHTS

- The compressive strength of the basalt fibre SCC was diminished by 28% at 500 °C.
- The splitting tensile strength of the SCC was increased by adding 0.25% of fibre.
- Considerable degradation in the flexural strength of fibrous SCC was seen at 300 °C.
- Slant shear of hybrid concrete was highly affected by fibre content of overlay.
- Interfacial surface roughened by sand blast provided proper bond in hybrid sample.

ARTICLE INFO

Article history:

Received 28 July 2020

Received in revised form 28 October 2020

Accepted 13 November 2020

Available online 19 December 2020

Keywords:

Basalt fibre concrete

Slant shear strength

Self-compacting fibre concrete

Fire impact on concrete

ABSTRACT

Basalt fibres are modern inorganic concrete fibres, fabricated by melting the basalt rock. These fibres exhibited remarkable resistance to elevated temperatures in comparison with other manufactured fibres. Thus, when the impact of fire is the main consideration, basalt fibres are favoured in the construction of concrete buildings. In this study, the effects of basalt fibres on the workability of fresh self-compacting concrete (SCC) were measured using slump flow, J-ring flow, V-funnel flow and L-box height ratio. The properties of hardened concrete such as compressive strength, splitting strength, modulus of elasticity, flexural strength, and Poisson's ratio were examined at temperatures between 25 °C and 500 °C. Also, the bond strength between the basalt fibre SCC as an overlay material and a normal concrete substrate was analysed at elevated temperatures. The interfacial surface between the concrete parts of the hybrid samples was roughened in different ways to determine the best roughening mode, which induced high slant shear strength of concrete under fire. The experimental results revealed that increasing the temperature up to 500 °C reduced the tensile and compressive strengths of SCC by over 20%. The optimum slant shear strength of hybrid concrete under fire was achieved by roughening the interfacial surface through the sandblasting method.

© 2020 Elsevier Ltd. All rights reserved.

1. Introduction

The consumption of concrete as construction material has increased continuously in recent years due to the rapid development of infrastructures [1]. Concrete has many merits, such as formability, durability and high mechanical strength. Hence, this stone-like material has advantages over other regular building materials. However, concrete has low strain capacity and tensile strength [2–4].

Non-metallic materials, such as fibre-reinforced polymers, have a suitable long-range potential because they are non-magnetic and non-corrodible, and their modulus of elasticity is lower than that of steel fibres. Consequently, these polymers are insensitive to shrinkage, anchorage and creep losses. Fibre-reinforced polymers are a suitable alternative to conventional concrete fibres because of their manufacturing and utilisation characteristics. Various types of fibres, such as cellulose, asbestos, polypropylene, steel, carbon, aramid, polyethylene, glass, polyvinyl alcohol and basalt, have been developed to reinforce concrete products [5]. Basalt fibres originated from basalt volcanic rocks that broke down into small particles and formed into continuous or chopped fibres [6]. These fibres have good resistance to elevated temperatures, impact

* Corresponding author.

E-mail addresses: james.haido@uod.ac (J.H. Haido), btayeh@iugaza.edu.ps (B.A. Tayeh).

actions and chemicals. Basalt fibre composites can be applied in insulation systems for sound and heat, soil strengthening, industrial flooring and rehabilitation of concrete structures. The production process of basalt fibres is similar to that of glass fibres; basalt rocks are quarried, mashed, washed with water and melted at 1500 °C. High-strength concrete can be achieved using fibrous self-compacting concrete (SCC) consolidates without any vibration. Fibrous concrete has a low yield value to guarantee high workability and an appropriate viscosity to prevent bleeding and segregation [7], and it can retain its homogeneity during placement to ensure sufficient durability of the structural members. Numerous studies have demonstrated that introducing fibres into SCC enhances SCC's mechanical properties, including toughness, compressive strength, tensile or flexural strength and impact resistance [8–14]. This concrete is usually characterised by low permeability, which plays a crucial role in repairing concrete that has deteriorated due to environmental factors. Structural safety and functionality are considerably affected by the bond between deteriorated concrete members and newly overlaid repairing materials. Effective bonding and reasonable permeability are required at the interface between old and new concrete to improve the resistance of the interfacial surface against the penetration of harmful chemicals. The latest generation of fibre polymer composites has elicited the interest of the research community and construction industry. Many studies [15–20] have revealed that the addition of basalt fibres is important in reducing the brittleness of concrete and improving its rupture modulus, deformation resistance, toughness and tensile strength. Several studies [21–24] have concluded that basalt fibres exhibit high resistance to tensile actions, impact loads, fatigue, thermal instability, corrosion and water penetration in comparison with carbon and glass fibres. Other studies [21,25,18] have examined the durability, thermal resistance and acoustic insulation of concrete with basalt fibres. These properties of concrete are considerably improved by the introduction of basalt fibres.

The mechanical properties of hybrid concrete fabricated with ordinary and high-strength concrete were investigated by Tayeh et al. [26–29], Denarie [30], Harris [31], Sarkar [32] and Santos and Julio [33]. These researchers used different roughening modes for the interfacial surface. Although basalt fibre concrete has many advantages, studies on its mechanical properties are limited [4,16,34–39]. Research that considered this concrete's behaviour at elevated temperatures is particularly scarce. In addition, the effect of using basalt fibre SCC as a repairing material on the strength of hybrid concrete composed of deteriorated ordinary concrete and high-strength basalt fibre SCC under fire is inconclusive. The current study investigated the properties (i.e. compressive strength, flexural resistance, Poisson's ratio and modulus of elasticity) of basalt fibre SCC at high temperatures. The slant shear strength at fire of hybrid concrete made with ordinary concrete substrate and basalt fibre SCC overlay was studied in consideration of various roughening modes of the interfacial surface between concrete parts.

2. Materials and methods

SCC was fabricated using ordinary Portland cement, and its properties are presented in Table 1. Grey silica fume, whose physical and chemical characteristics are listed in Table 2, was used as a pozzolanic material to improve the strength of this concrete. Crushed coarse aggregate and river sand were also utilised for grading (Fig. 1) in compliance with ASTM C127 [40] and C128 [41]. High-performance basalt fibres (Fig. 2) were used in SCC manufacturing; the average diameter and length of these fibres were $16 \pm 2 \mu\text{m}$ and 24 mm, respectively. A polycarboxylic polymer

Table 1
Properties of the ordinary Portland cement used in this study.

Chemical compositions	
Item	Magnitude
CaO	62.15%
SiO ₂	18.94%
Al ₂ O ₃	3.90%
Fe ₂ O ₃	4.77%
MgO	1.52%
SO ₃	2.37%
Loss on ignition	2.18
Insoluble residue	0.65
Physical properties	
Property	Value
Specific gravity	3.15
Specific surface area	338 m ² /kg
Initial setting time	181.7 min
Final setting time	255 min

Table 2
Characteristics of the silica fume used in this study.

Item	Value
Specific gravity	2.2
Specific surface area	369 m ² /kg
SiO ₂	greater than 90%

hyperplast superplasticizer with a light-yellow colour was also utilised in SCC production to achieve workability and improve strength. The specific gravity of this liquid is 1.05 ± 0.02 .

Concrete mixtures (Table 3) were designed in accordance with the desired compressive strength at the age of 28 days. Four dosages of basalt fibres, namely, 0%, 0.25%, 0.5% and 1.0%, were utilised in the mixtures. Noticeably, the density of concrete or the amount of mass incorporated into the unit volume of SCC decreased with incorporating basalt fibres. Accordingly, the density of the hardened SCC concrete M1, M2, M3, and M4 recorded 2340, 2320, 2290, and 2265 kg/m³, respectively. The workability of the fresh SCC was measured using slump flow diameter, V-funnel flow time, L-box height ratio and J-ring in terms of flow diameter and time in accordance with EFNARC [42] and ASTM C1621 [43]. Slump test was used as the primary check to describe the workability performance of SCC mixtures and their flowability characteristics of SCC. The diameter of the fresh SCC was measured based on EFNARC [42] in two directions as shown in Fig. 3 and the average diameter was given as slump flow diameter. Also, the SCC viscosity was measured in terms of slump flow time (T_{50}), which is the time required for fresh concrete to form a circle with a diameter of 50-cm. V-funnel flow test (Fig. 3). It was used to describe the indirect viscosity characteristic of the SCC mixtures based on the flowing rate as given in EFNARC [42]. The time measured in the V-funnel flow test is the elapsed time between the beginning and end of flowing of SCC from the funnel. To assess the segregation in the SCC mixtures, the V-funnel flow time test was repeated after the test was conducted first. The workability of fresh concrete was also checked via L-box test (as shown in Fig. 3) according to EFNARC [42], whereby the fresh SCC in the vertical box was allowed to flow through the rebars to the horizontal box. When the flowing of the mixture stopped, the height ratio (h_2/h_1) was determined to evaluate the passing ability performance of SCC. The J-ring flow test was performed by using a specific apparatus with a ring with rebars (as shown in Fig. 3) as recommended by ASTM C1621 [43]. The flow diameter of the SCC mixture was measured to assess its passing ability and flowability.

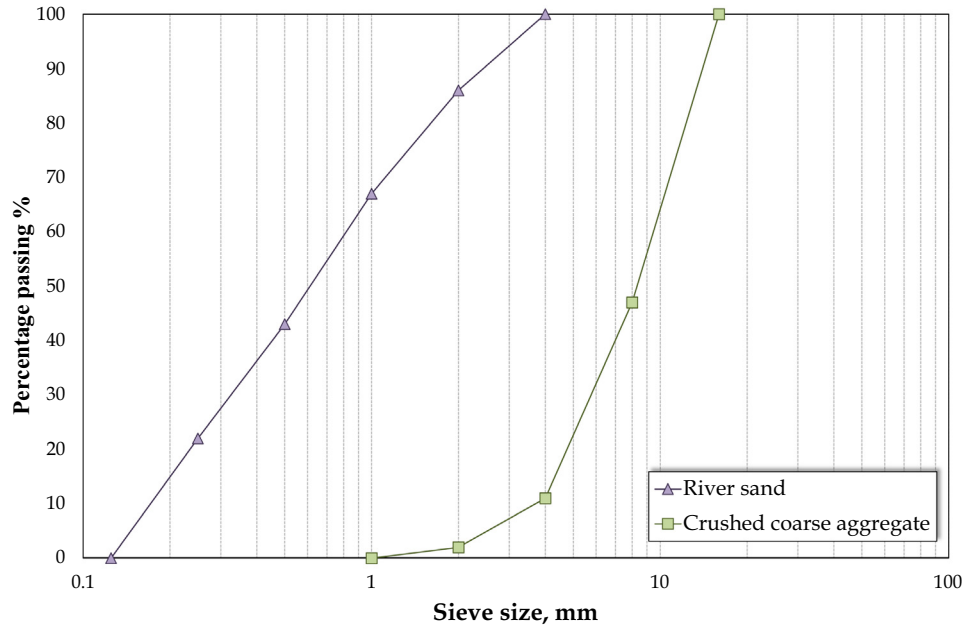


Fig. 1. Sieve analysis of the used aggregate.



Fig. 2. Basalt fibres used in this study.

The average compressive strength was tested using cylindrical specimens (as shown in Fig. 4) with a height of 200 mm and a diameter of 100 mm in accordance with ASTM specifications [44]. Three specimens were selected for each SCC mixture, and the compression test (Fig. 4) was carried out under laboratory conditions after specimens were exposed to an elevated temperature

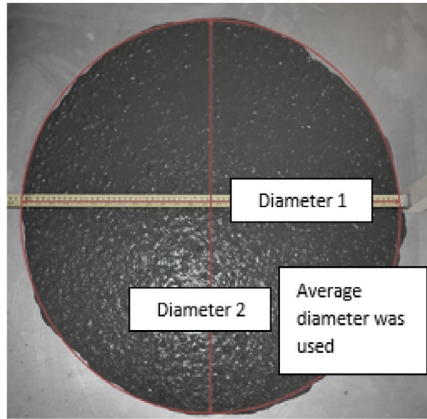
in a furnace (Fig. 4) up to 500 °C. All the samples were tested at the age of 28 days, started after cooling them at a laboratory temperature of 20 °C. The compressive strength of these specimens was measured in a compression testing machine (Fig. 4) with a capacity of 3000 kN. The elastic modulus of the SCC cylinder, with a size of 100 mm diameter and 200 mm height, was measured based on the stress–strain relationship as given in the testing procedure following ASTM C469 standards [45]. The test was performed on three specimens and their average was submitted as the result of this modulus for each SCC mixture. Furthermore, since the main objective of this study is to investigate the temperature effect on the mechanical properties of the SCC mixtures, the elastic modulus was determined for specimens aged 28 days at the temperature range of 20–500 °C. The exposure temperature–time relationship was established as depicted in Fig. 5. Hence, this elevated furnace temperature was applied to the samples within 150 min, ending with a homogenous temperature equivalent to that of the lab.

Besides, the Poisson's ratio of the SCC specimens was measured at high temperatures following the regulations provided in ASTM standards [46]. Cylindrical specimens were utilized, with a size similar to that of the compression test specimens, to determine this ratio. The Poisson's ratio test was carried out for three specimens and the average ratio was selected for each SCC mix. Axial and lateral strains were recorded to compute the Poisson's ratio by using two strain gauges positioned on the specimen (as shown in Fig. 6) orthogonally to each other. The specimens were subject to the elevated temperature prior testing considering the procedure given in the compression test.

The tensile strength of SCC was investigated via a three-point flexural test based on the ASTM standard methodology [46,47].

Table 3
Mix design of the present SCCs.

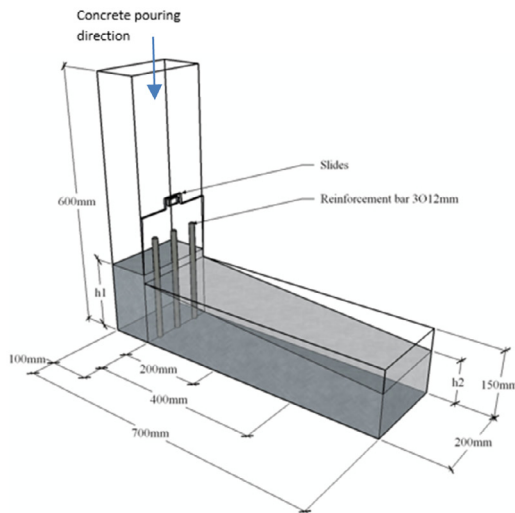
Mix ID	Cement (kg/m ³)	Silica fume (kg/m ³)	Water (kg/m ³)	Sand (kg/m ³)	Coarse aggregate (kg/m ³)	Basalt fibre (kg/m ³)
M1	484.5	85.5	171.0	936.3	671.7	0.0
M2	484.5	85.5	171.0	936.3	671.7	7.0
M3	484.5	85.5	171.0	936.3	671.7	14.0
M4	484.5	85.5	171.0	936.3	671.7	28.0



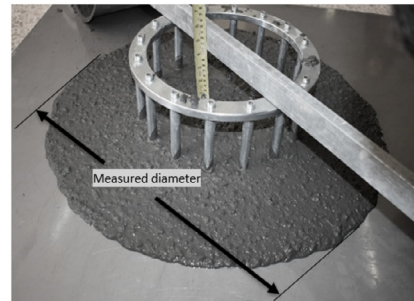
a- Slump test measurement



b- V-funnel test setup



c- L-box instrumentation



d- J-ring flow test

Fig. 3. Part of the workability tests for the SCC concrete.



a- SCC cylinders



b- samples in furnace



c- sample testing

Fig. 4. Compression test procedure of SCC.

The size of the specimens for the flexural test (as shown in Fig. 7) was $100 \times 100 \times 400$ mm prisms. The average tensile strength was determined for every three samples, with an age of 28 days, subjected to elevated temperatures of 200–500 °C. The flexural test

was performed at room temperature after the samples had cooled down.

The permeability of the SCC was tested using water and chlorite penetration depths in accordance with TS EN-12390-8 [48] and

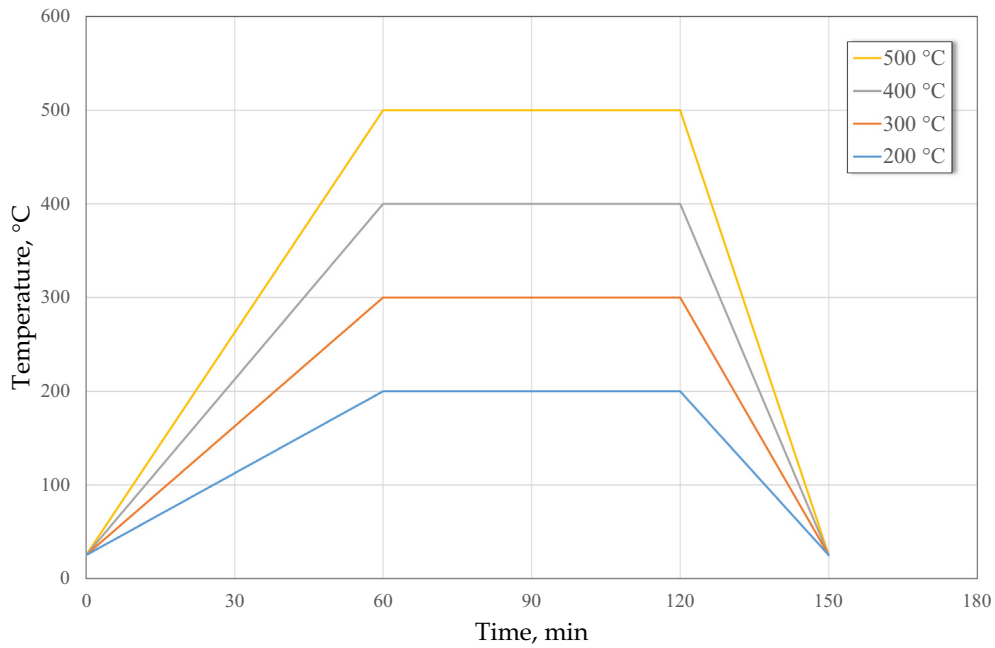


Fig. 5. Time history of the applied temperature.

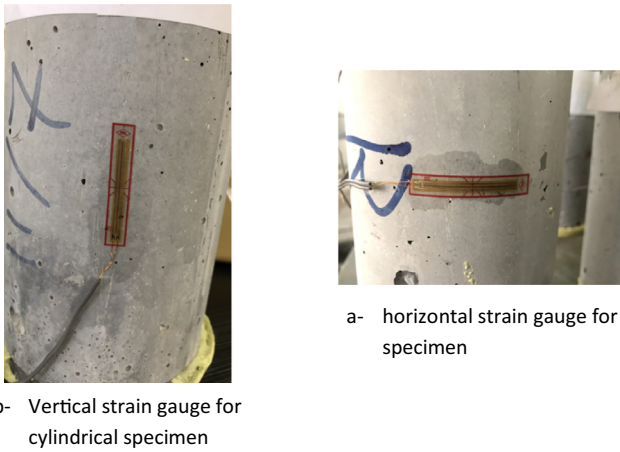


Fig. 6. Sample preparation for Poisson's ratio testing.



Fig. 7. Flexural test of the SCC prisms.

ASTM C1202 [49] standards, respectively. Accordingly, water passing deep through the concrete capillary pores was measured in the permeability test. Cylindrical specimens (dimension: 100 mm diameter and 200 mm height), as shown in Fig. 8, were adopted in the water permeability test. The specimens were dried at an oven temperature of 50 ± 5 °C before testing based on the TS EN-12390-8 criteria [48] to attain a constant mass of the specimens. Part of the specimen was used in the test with the size of 100 mm diameter and 50 mm height. The testing set up for these specimens' underwater pressure is depicted in Fig. 8. Chloride penetration test was performed utilizing the SCC cylinders with the same dimensions given in the water permeability experiment according to ASTM C1202 [49]. The specimen was separated into three parts, including the top and bottom parts of the SCC cylinder that were selected for the chloride sorptivity test, whereas the middle part was utilized in rapid chloride permeability testing. The average permeability was determined considering the results of these three specimens, which were cured in water for 28 days

before testing. Testing was carried out using contained cells (Fig. 8); where the specimens were placed in these containers between sodium chloride (NaCl) and sodium hydroxide (NaOH). The specimens were subject to a direct electrical current of 60 V for 6 h. Consequently, the charge passing through the SCC specimen was recorded in coulombs using the Simpson's integration approach. The results of these experiments can help in assessing the suitability of the basalt fibre SCC as a repairing overlay material for hybrid concrete specimens.

The wooden molds were employed in the preparation of prismatic hybrid concrete specimens for the slant shear strength test. These specimens, with the size of 300 mm, 100 mm and 100 mm, were produced by ordinary concrete representing old concrete substrate part and SCC referring to new overlay concrete [50–52]. The old concrete part represents the deteriorated concrete and the

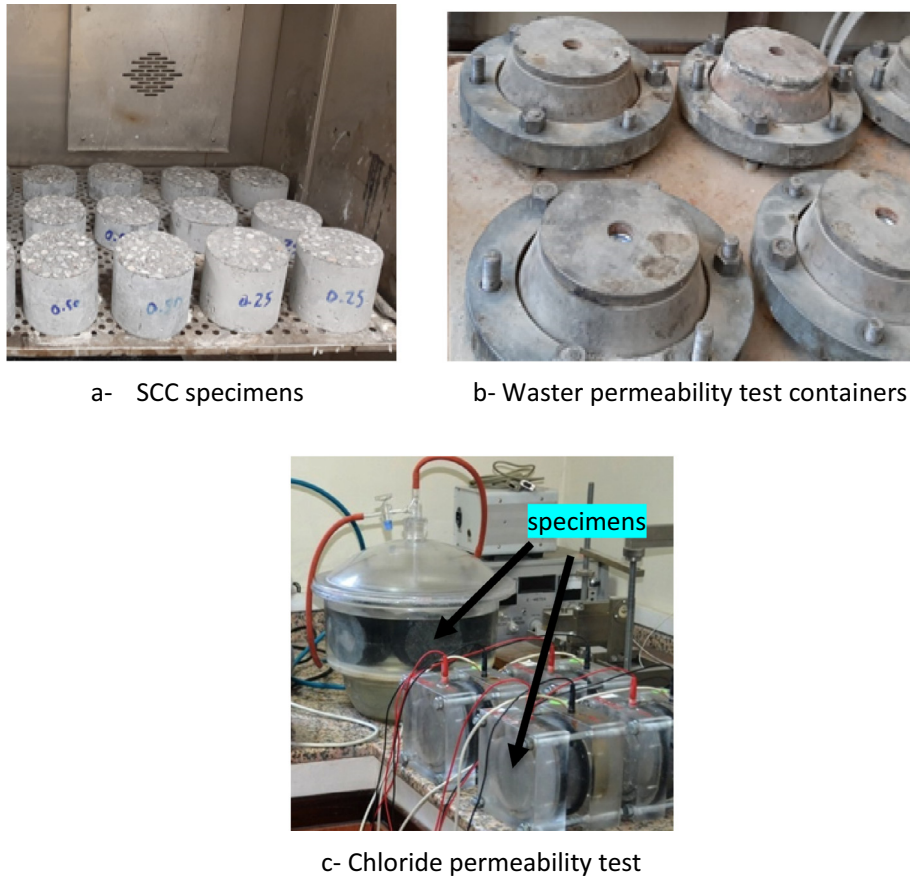


Fig. 8. Permeability test of the SCC specimens.

new SCC part refers to the new concrete-repairing part. Motor oil was used to paint the molds before concrete casting to inhibit the adhesion between concrete and the wooden mold. The conven-

tional concrete or the substrate part (as shown in Fig. 9) was cast first in a mould in two layers; each concrete stratum was rodded by 25 blows to achieve the desired compaction. An ordinary concrete mix for the substrate was designed for compressive strength of 30 MPa following the ACI 211 criteria [53]. The interfacial surface on the normal concrete part was roughened after 28 days of water curing. Four surface roughening modes (Fig. 10); namely, as-cast (control), sandblasted, drilled with holes and grooved, were adopted. Subsequently, the specimens were re-moulded after two months to cast the overlay or repairing part of high-strength SCC to form the specimens (Fig. 11) for the slant shear test. The slant shear strength of the hybrid concrete was determined to examine the degree of bonding between the old and new concrete parts, thereby checking the efficiency of SCC overly in providing appropriate strength in combination with ordinary concrete. ASTM C882 [54] was used in the current slant shear strength test considering the firing effect at 20–500 °C. Accordingly, the specimens were exposed to a furnace temperature provided in Fig. 5 before testing. The strength of the hybrid concrete was computed as hereunder:

$$F_{slant} = \text{Applied load at failure} / \text{inclined area of the interfacial surface} \quad (1)$$

Scanning electron microscopy (SEM) was employed in present study to reveal the microcracks in the two parts of the hybrid concrete. The perfect bond on the interfacial surface was confirmed through this procedure. The distribution of basalt fibres in the overlay stratum was observed using SEM specimen (Fig. 12) with a length of 4 cm, width of 2 cm and thickness of 2 cm.

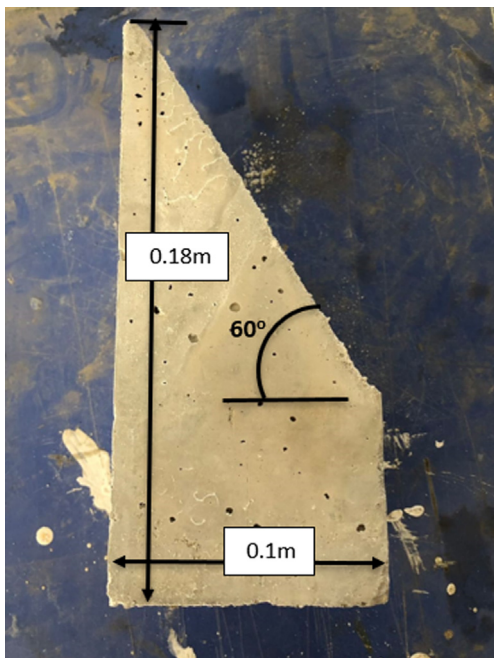


Fig. 9. Ordinary concrete substrate part of the hybrid concrete specimen.

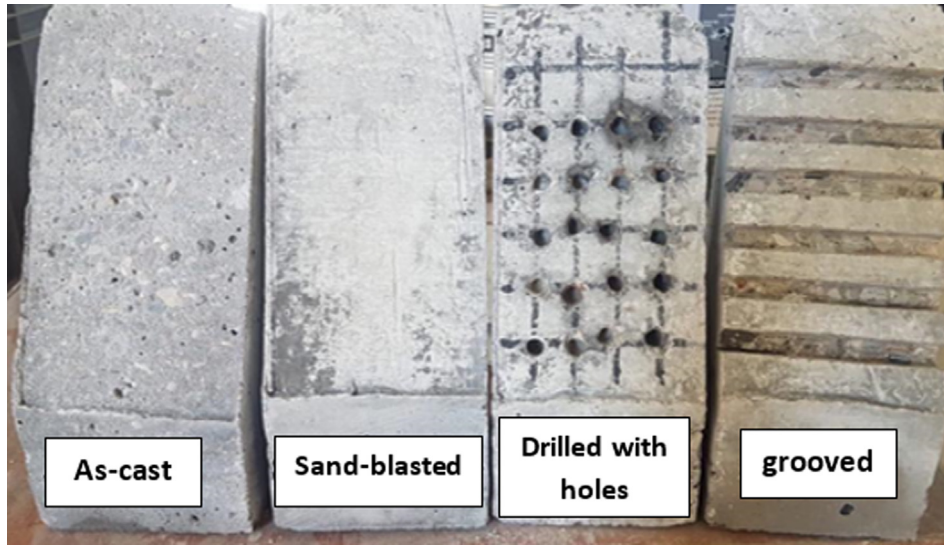


Fig. 10. Roughened interfacial surfaces of the hybrid concrete samples.

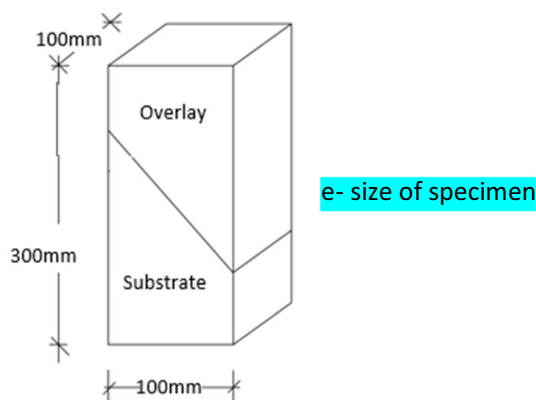
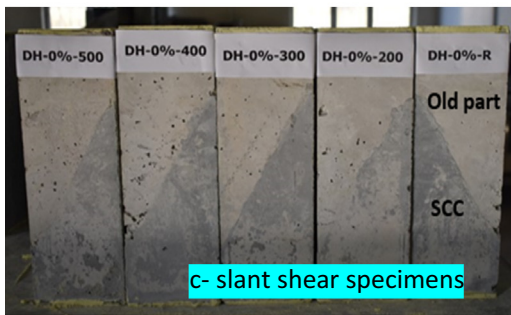
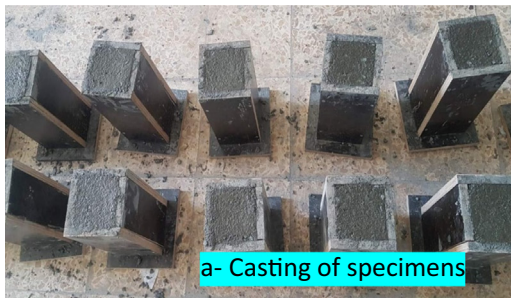


Fig. 11. Preparation of specimens for slant shear test.

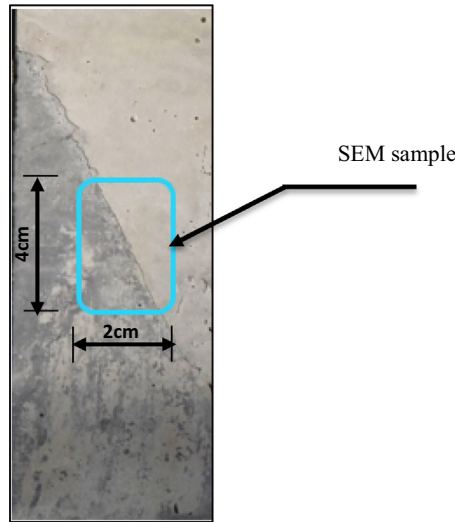


Fig. 12. SEM sample for the hybrid concrete.

3. Results and discussion

3.1. Workability tests

3.1.1. Slump flow diameter

The outcomes for slump flow test for fresh SCC are given in Table 4. Slump flow diameter of 0.74 m was noticed for SCC without fibres which can be classified as SF2 class of concrete flow based on EFNARC specifications [42]. This class of concrete can be used in the construction of walls and columns. In addition, results indicated that the introduction of basalt fibres in fresh SCC degraded its flow. The utilization of basalt fibre content of 0.25% is considered the inflection point at which the flowability of SCC changes from SF2 class to SF1 with respect to the current results. More specifically, a dramatic decrease was observed in the slump flow diameter (less than 0.65 m) of the SCC incorporating fibres with volume fraction of 0.50–1.00%. This performance is expected of the SCC flowability with the utilization of natural basalt fibres, whereby a similar pattern in the findings was obtained in previous studies [6,16,18] as illustrated in Table 4. This reduction in workability is attributed to absorbing of a part of mixing water by micro-scale particles for fibres which resulting in increasing the cohesiveness of fresh concrete. The uncertainty analysis of the workability data, listed in Table 4, showed that a minimal divergence in the data was obtained in the L-box workability test despite using different fibre contents in SCC.

3.1.2. J-ring Flow diameter

J-ring flow diameter test was also conducted in this study to show the robustness and reliability of the flowability test records.

Table 4
Workability test results for SCC.

Fibre content (%)	Slump flow diameter (m)	J-ring diameter (m)	T50 slump flow time (s)	V-funnel flow time (s)	T50 V-funnel flow time (s)	L-box height ratio (h2/h1)	Slump* (m) [6]	VeBe* time (s) [16]
0	0.74	0.65	2.1	6	9	0.78	0.18	12
0.25	0.7	0.62	3.2	7.4	10	0.81	–	–
0.5	0.59	0.56	3.9	8.2	11.4	0.85	0.13	13
1.0	0.58	0.54	4.2	8.9	11.8	0.78	0.13	48
Uncertainty**	0.0398	0.0256	0.466	0.622	0.645	0.0166		

* these data are for ordinary concrete not SCC

** Uncertainty = $\sqrt{\frac{\sum(x_i - m)^2}{n(n-1)}}$; where xi = ith reading in data, m = mean of data and n = readings number

The correlation between SCC flow diameter and the used fibre volume fraction is illustrated in Table 4. These results are considered as a support for above-mentioned slump flow test. Similar trend in flowability performance for slump test was seen in J-ring flow test; where remarkable decrease in flow diameter was demonstrated with increasing the fibre content more than 0.25%. This decrement in flow is owing to absorption of water by the fibres such as that case in slump test. This test can also provide information on the passing performance of the SCC mixes because SCC flowed amongst the rebars. Decreasing the slump flow diameter worsened the flowing and passing capabilities.

3.1.3. T50 Slump flow time

The effect of the fibre content on the slump flow time of SCC was investigated as well. The increment in T50 slump flow time (Table 4) for SCC is comply with the reduction in the slump diameter. Accordingly, an increase of more than 52.38% in the flow time was noticed with increasing in the fibre volume fraction greater than 0.25%. This increasing in the flow time is due to the high cohesiveness resulted from the introduction of fibres. Based on these experimental data, the mixes of SCC provided in the current work can be sorted as VS2 viscosity class concrete conforming with EFNARC standards [42].

3.1.4. V-funnel Flow time

The viscosity of fresh SCC was measured indirectly via V-funnel flow test to find T50 slump and flow time according to EFNARC specifications [42]. Table 4 reveals that the results of both measurements for time were hassling in the direction of delaying of flow with increasing fibre content. These experimental observations are referring to that SCC with fibre content less than 0.25% is classified as VF1 viscosity class; and other mixes will be regarded as VF2 class with respect to EFNARC flow time standards. Thus, it can be deduced that the use of fibre content more than 0.25% can change not only the flowing class but also the viscosity class.

3.1.5. L-box height ratio

The passing capability of the fresh SCC was investigated in this testing work considering L-box height ratio experiment relying on the EFNARC instructions [42]. Test results are listed in Table 4 pointing out that average decrement of 7.58% was noted in height ratio of basalt fibre SCC in comparison to reference mix without fibres. According to EFNARC standards, SCC containing basalt fibre content lesser that 1.0% can be classified as PA2 passing class of capability.

All of the SCC mixtures, except for the SCC mixture produced with a basalt fibre volume fraction of 1.0%, could be classified under the passing capability class of PA2. Despite the fact that the SCC mix with fibre content $\geq 1.0\%$ did not fall in this passing capability class, the L-box height ratio of this mix was 0.78.

3.2. Mechanical tests

3.2.1. Compressive strength

The effect of high temperature and fibre dosage on the compressive strength of the SCC mixtures at the age of 28 days is illustrated in the Fig. 13. An average strength reduction of 11.43% was observed when the fibre content was increased. This result is attributed to the reduction in the workability and density of SCC caused by fibre introduction. In addition, Fig. 13 reveals that any change in the high temperature exerted a remarkable influence on the compressive strength of SCC, especially at temperatures exceeding 200 °C where an average strength reduction of 28% was demonstrated. This degradation in strength under fire was a result of the reduced cohesiveness of the SCC composites. The effect of exposure to a high temperature on the compressive strength of SCC was predicted by the uncertainty analysis, which refers to 2.65 MPa as an uncertainty value in the measurements. This great uncertainty can be attributed to the vulnerability of the basalt fibre SCC to an elevated temperature, which has led to degradation in the concrete strength. The axial strains were recorded during the compression test on the SCC cylinders, as illustrated in Figs. 14 and 15. A decrease in concrete compressive strain was observed in Fig. 14 when the temperature increased because of the onset of micro-cracks and concrete spalling. Fibre dosage exerted no remarkable effect on this strain, as depicted in Fig. 15, due to the reduction in the density and cohesiveness of concrete with high fibre content.

3.2.2. Elastic modulus

The elastic modulus of the basalt fibre SCC mixtures was investigated at high temperatures in consideration of different fibre volume fractions, as depicted in Fig. 16. Fibre dosage exerted a trivial effect as the modulus of elasticity values fluctuated. However, the elastic modulus of SCC had an opposite relationship with high temperature. The results confirmed that the highest modulus was achieved at a laboratory temperature of 20 °C, and the texture of SCC was considerably influenced by the increment in temperature. Increasing the temperature to up to 500 °C caused decrements of 36.6%, 36.3%, 44.8% and 34.0% in the elastic modulus of the SCC mixtures manufactured with basalt fibre volume fractions of 0%,

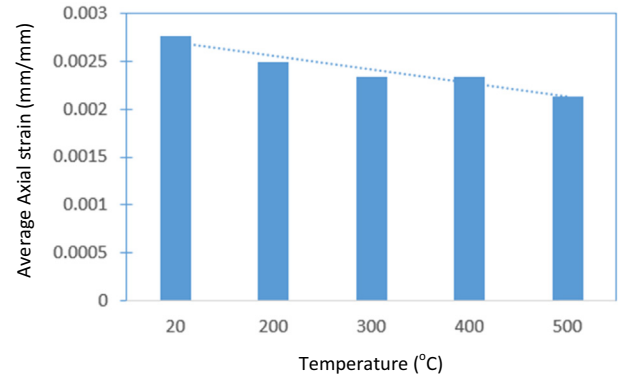


Fig. 14. Effect of elevated temperatures on the average axial compressive strain of the SCC mixtures considering fibre content of 0–1%

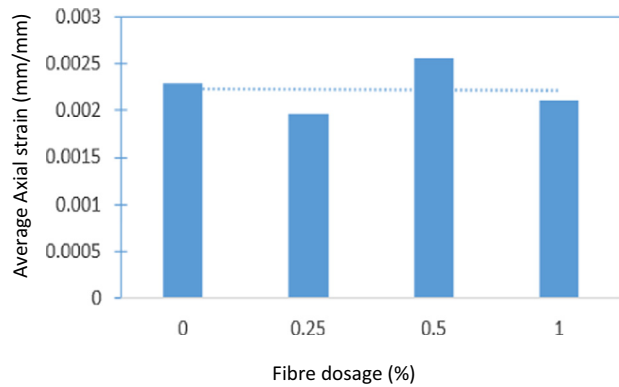


Fig. 15. Influence of basalt fibre content on the average axial compressive strain of the SCC mixtures at temperature of 20–500 °C.

0.25%, 0.50% and 1.00%, respectively. Poisson’s ratio was also measured for the SCC mixtures at different temperatures, as shown in Fig. 17. The results indicated that temperature exerted a slight

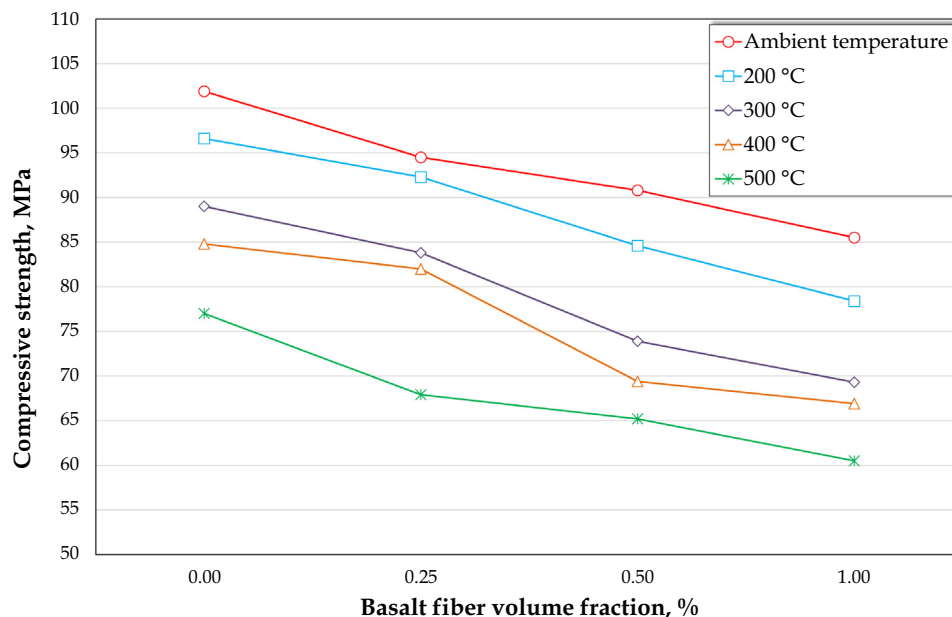


Fig. 13. Compressive strength of the SCC mixtures with respect to high temperature and basalt fibre content.

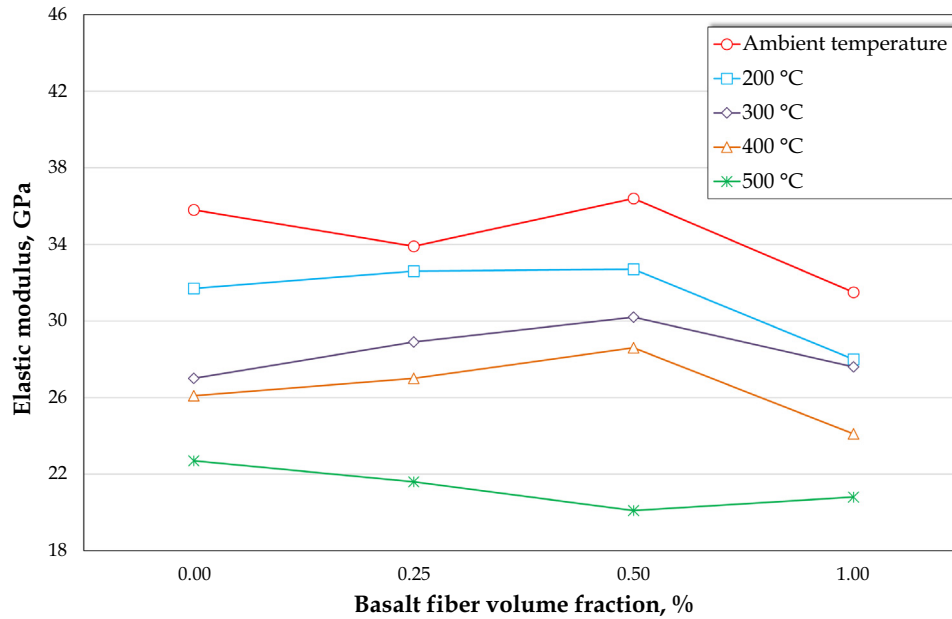


Fig. 16. Elevated temperature and fibre content effect on the elastic modulus of the SCC mixtures.

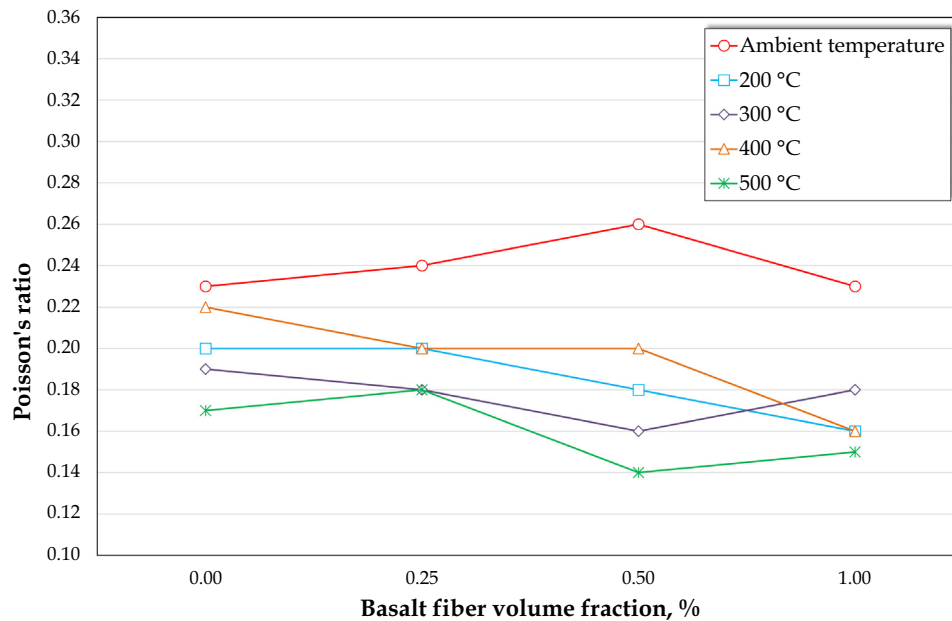


Fig. 17. Influence of temperature and fibre content on the Poisson's ratio of the SCC mixtures.

effect on Poisson's ratio, as evidenced by the slight lateral deformation of the concrete samples under loading. The ratio exhibited an increasing trend, but it was maintained at the laboratory temperature with a basalt fibre volume fraction of up to 0.50% due to the further reduction in the density and cohesiveness of SCC when a high fibre content was used.

3.2.3. Splitting tensile strength

Given that measuring the direct tensile strength of concrete is difficult, the tensile strength of concrete is usually measured through either splitting tensile or flexural strength tests. In the current study, splitting tensile and flexural strength tests were conducted to achieve supporting information on the influence of basalt fibre on the tensile behaviour of the SCC mixtures. The

results obtained from the splitting tensile strength test are presented in Fig. 18. The splitting tensile strength of the SCC mixtures increased when 0.25% basalt fibre was added, but it decreased when more than 0.25% basalt fibre volume fraction was added. This result may be caused by the decrement in the self-compactability of the concrete resulting from the incorporation of the high basalt fibre content. Another reason may be the coagulation of basalt fibre particles at high volume fractions. At ambient temperature, the highest splitting tensile strength value of 7.32 MPa was achieved in the SCC mixture manufactured with 0.25% basalt fibre. The lowest value of 6.56 MPa was obtained in the SCC mixture produced with 1.00% basalt fibre. The basalt fibre with a macro-scale particle diameter may not have been well distributed in the cement matrix. Hence, the splitting tensile strength decreased after the 0.25% vol-

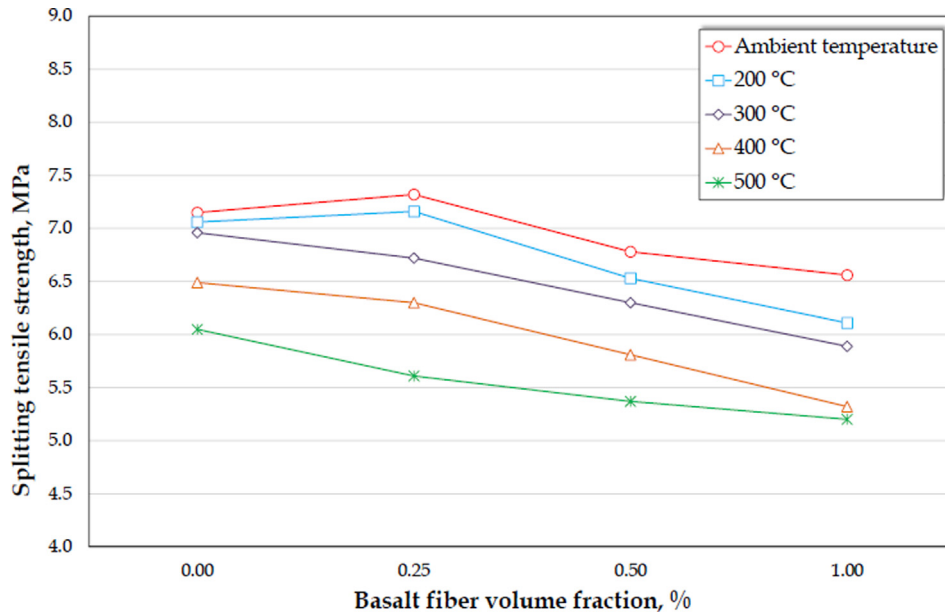


Fig. 18. Variation in the splitting tensile strength of the SCC mixtures with respect to the basalt fibre volume fraction and temperature.

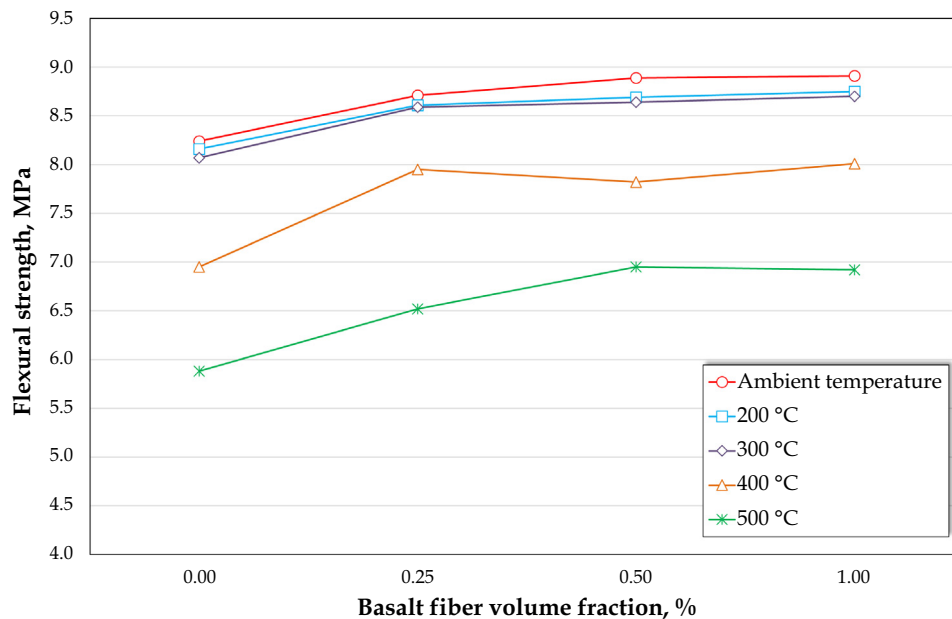


Fig. 19. Modulus of rupture (flexural strength) of the SCC mixtures.

ume fraction. Basalt fibre with more than 1.0% volume fraction should be used to achieve good tensile performance.

3.2.4. Flexural strength

The flexural strength of the SCC samples was recorded with respect to the combined influence of basalt dosages and applied temperature changes (Fig. 19). The measurements showed that the flexural strength of SCC increased by as much as 8% when the fibre content was increased to 1.00%, and it decreased when the temperature was increased. This result confirms the promising role of basalt fibres in arresting micro-cracks in concrete and improving concrete’s tensile strength. In addition, an average reduction of 24.45% in flexural strength was observed when the exposure temperature was increased from 20 °C to 500 °C due to the fragility of concrete under elevated temperatures. With regard

to the water penetration of SCC, the sorptivity coefficient was measured in relation to the used fibre volume fraction. A large reduction of 35.56% in the sorptivity coefficient was observed when the fibre contents were increased from 0% to 1.0%. This feature plays a crucial role in providing a proper basalt fibre SCC repairing material. The permeability of SCC was also examined in terms of the chlorite ion penetration depth. An average decrease of 28.57% was observed when a fibre content of 1.0% was utilised.

3.2.5. Slant shear strength

The slant shear strength of the hybrid concrete, which was composed of ordinary concrete substrate and high-strength SCC overlay, is shown in Figs. 20–23. Three parameters, namely, fibre dosage, high-temperature changes and roughening mode of the interfacial surface between old and new concrete parts, were con-

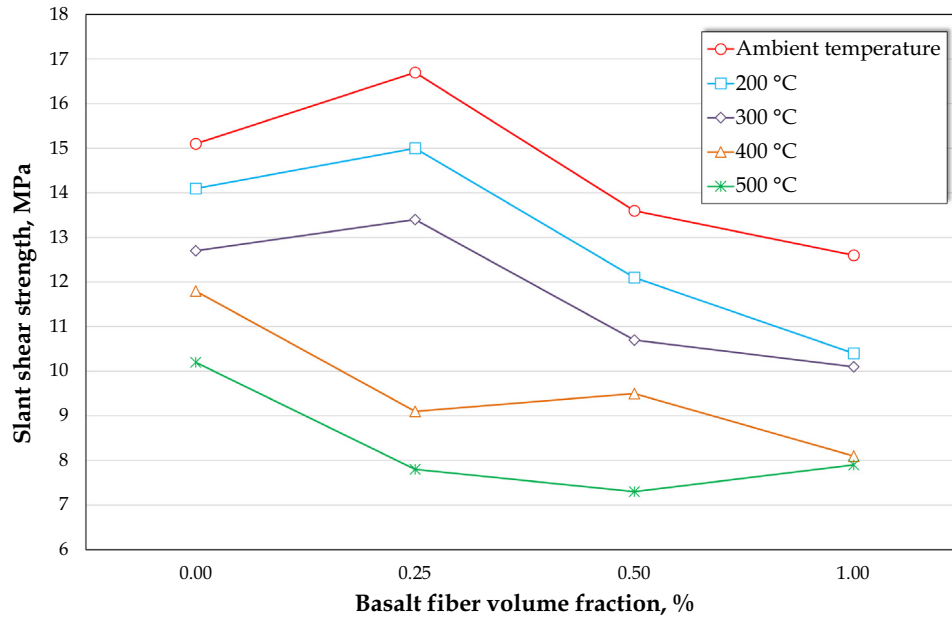


Fig. 20. Slant shear strength of the hybrid concrete with an as-cast interfacial surface.

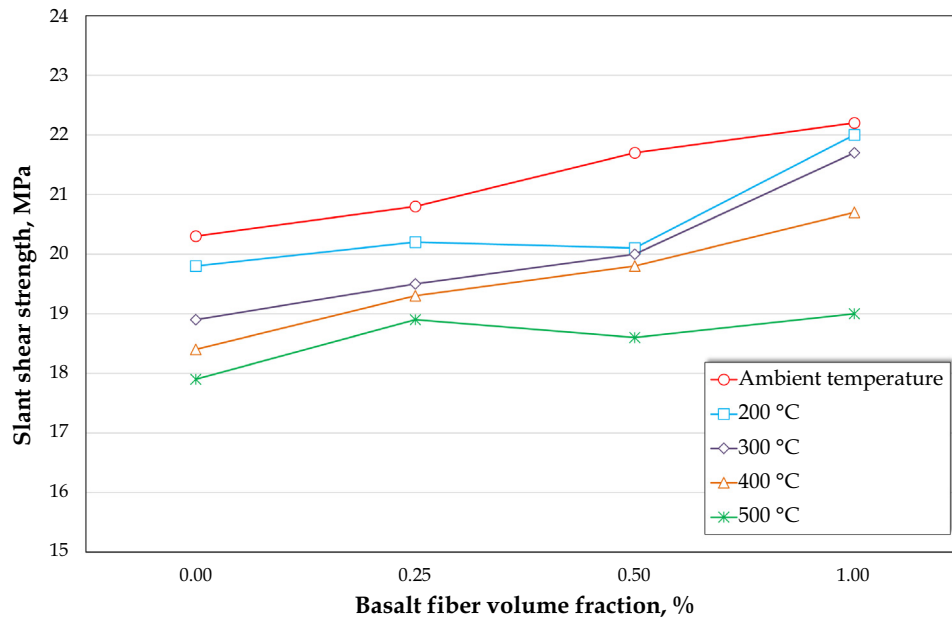


Fig. 21. Slant shear strength of the hybrid concrete with the interfacial surface roughened with holes.

sidered in measuring this strength. Low slant shear strength values were obtained in the control or as-cast hybrid concrete with high basalt fibre content of the SCC overlay due to the increased brittleness of this concrete part. Moreover, an increase in the slant shear strength was observed in Fig. 20 for the SCC incorporating 0.25% fibre due to the slight effect of temperature ≤ 300 °C on the brittleness change between the substrate and overly. The increase in temperature beyond 300 °C has an insignificant role in degrading the strength (Fig. 20) of the SCC with fibre content $\geq 0.25\%$ due to the weakness in the interfacial surface and cohesiveness of overly of the hybrid specimens. Generally, the slant shear strength of hybrid concrete samples with a roughened interfacial surface is enhanced by introducing overlay concrete with high fibre content. An ascending trend (Fig. 21) was found in the slant shear strength

of hybrid concrete, with interfacial surface roughened by holes, with increasing the fibre content. The reason for this behaviour is the appropriateness in the bond between old and new concrete parts despite the exposure to a high temperature. Higher strength was obtained (Fig. 22) by using the grooved interfacial surface instead of holes due to the improvement in the interlock between these concrete parts at the interfacial surface, resulting from groove configuration. A proper slant shear strength of hybrid concrete can be achieved by utilising a sand-blasted interfacial surface, which provides significant frictional resisting force on the plane and a minimal reduction in strength even under increasing temperatures. Based on these results, the recommended fire resistance of hybrid concrete is 2.5 h. The following modes of failure of the hybrid concrete under applied loading were observed: columnar

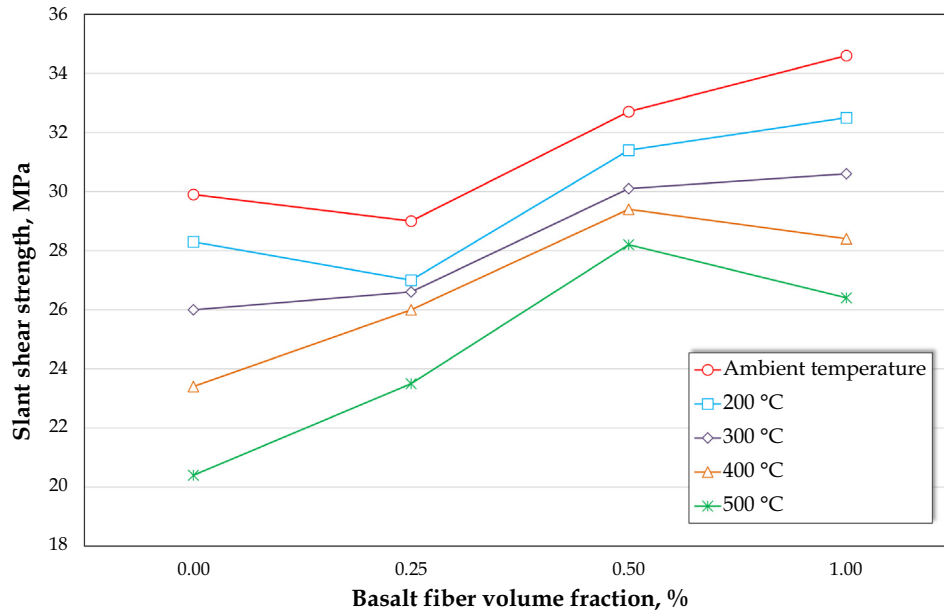


Fig. 22. Slant shear strength of the hybrid concrete with a grooved interfacial surface.

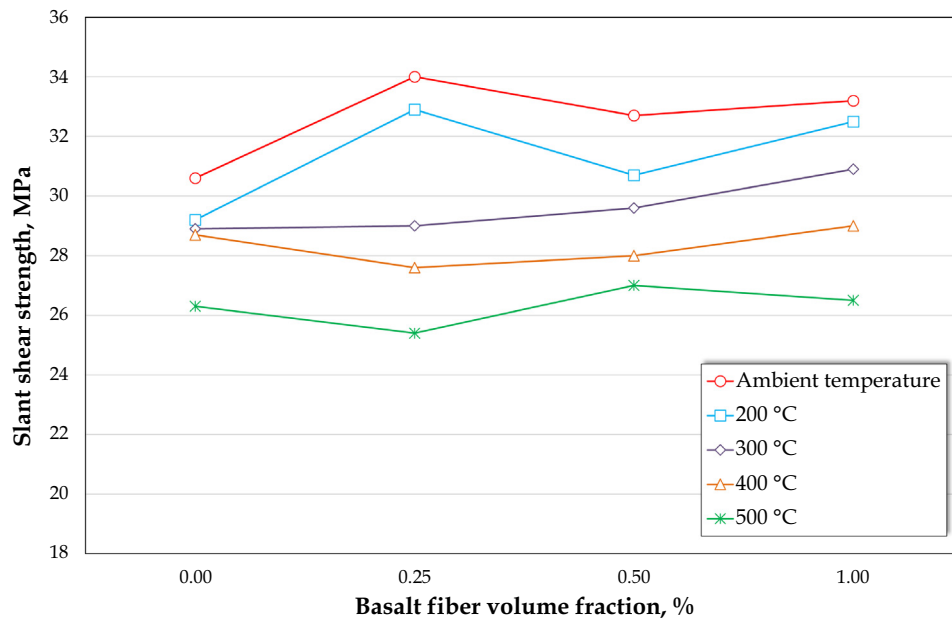


Fig. 23. Slant shear strength of hybrid concrete with a sand-blasted interfacial surface.

failure (CF), overlay part failure (OL), substrate part failure (SL) and interfacial surface failure (IF). The CF mode in hybrid concrete is an indication of a perfect bond between two parts of hybrid concrete. The worst failure mode is IF, which results from the de-bonding of concrete parts. These failure modes of the current hybrid concrete samples are given in Fig. 24 and Table 5. A fibre dosage of more than 0.25% led to the collapse of the hybrid concrete via SL because of the difference in rigidity between the high-stiffness overlay and low-rigidity substrate. The micrograph (Fig. 25) of the SEM test was used to examine the microstructure of the transition area between normal and basalt fibre samples of the hybrid concrete without IF. SEM samples were obtained from the hybrid concrete specimens tested previously in the slant shear experiment. The micrographs revealed that the overlay concrete remained intact, with insignificant cracks spreading towards the interfacial surface.

A superior bond was demonstrated by the hybrid concrete samples with sand-blasted and grooved interfacial surfaces to some extent. This feature is noticeable in Fig. 24, which shows that microcracks were induced in the normal concrete substrate part. The excellent permeability of the high-strength basalt fibre SCC played a remarkable role in enhancing the bond strength of the interfacial surface of the hybrid concrete samples [55]. Accordingly, good adhesion and superior interlock were achieved between the old and new concrete segments.

3.2.6. Statistical analysis

The mechanical properties of basalt fibre SCC were correlated with the volume fraction of fibres, high temperature change and roughening mode of the interfacial surface of hybrid concrete (independent parameters). Thus, the impact or statistical significance

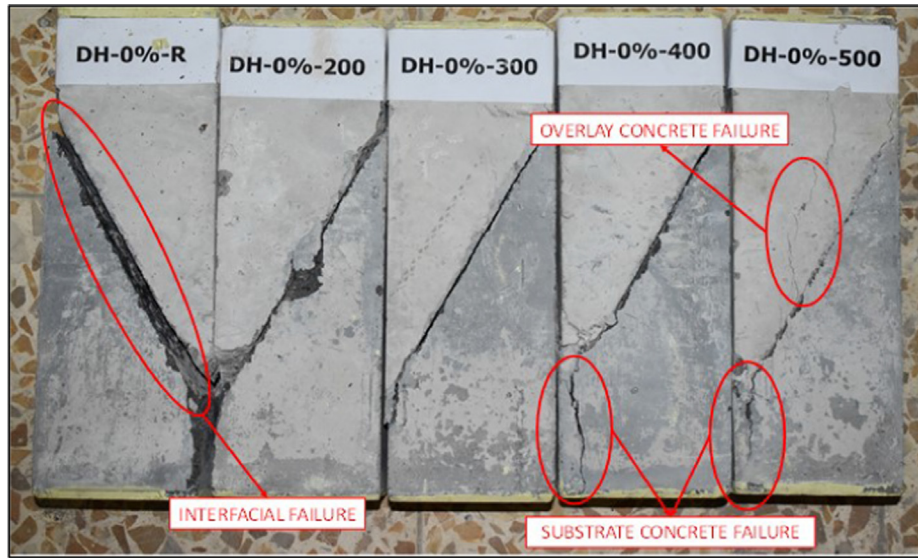


Fig. 24. Modes of failure in the hybrid concrete specimens.

Table 5
Failure modes of the hybrid concrete at elevated temperatures.

Surface preparation type	Temperature(°C)	Mix ID	M2	M3	M4
		M1			
As-cast	25	IF and OL	IF and OL	IF, OL and SL	IF, OL and SL
	200	IF and OL	IF and OL	IF, OL and SL	IF, OL and SL
	300	IF and OL	IF and OL	IF, OL and SL	IF, OL and SL
	400	IF and OL	IF and OL	IF, OL and SL	IF, OL and SL
	500	IF and OL	IF and OL	IF, OL and SL	IF, OL and SL
Drilled with holes	25	IF, OL and SL			
	200	IF, OL and SL			
	300	IF, OL and SL			
	400	IF, OL and SL			
	500	IF, OL and SL			
Grooved	25	OL and SL	SL	OL and SL	OL, SL and CF
	200	OL and SL	SL	IF, OL and SL	OL, SL and CF
	300	OL, SL and CF	SL and CF	IF, OL and SL	CF
	400	SL	SL and CF	SL	SL
	500	SL	IF-OL-SL	SL	SL and CF
Sand-blasted	25	SL and CF	IF, OL and SL	IF, OL and SL	IF and OL
	200	OL, SL and CF	IF, OL and SL	IF, OL and SL	OL, SL and CF
	300	OL, SL and CF	OL and CF	IF, OL and SL	OL, SL and CF
	400	OL, SL and CF	SL and CF	OL and SL	SL
	500	OL, SL and CF	SL	SL	IF, OL and SL

of each parameter on the resulting strength of the basalt fibre SCC samples should be predicted through ANOVA. The general linear model (GLM-ANOVA) was used in the present statistical evaluation. Table 6 indicates that high temperature had a more remarkable effect on the mechanical properties of homogenous basalt fibre SCC compared with the other parameters. With regard to hybrid concrete, ANOVA (Table 6) revealed that roughening mode of the interfacial surface exerted a larger effect on slant shear strength compared with high temperature. Furthermore, the normalization of the experimental data of the mechanical properties of SCC and hybrid concrete was carried out as illustrated in Figs. 26 and 27 with respect to the laboratory temperature. The outcomes of Fig. 26 revealed that the vulnerability of the Poisson’s ratio of SCC, to an elevated temperature, is higher than that of other properties in terms of the mean value. This magnitude is equivalent to the average ratio of property at an elevated temperature to that of the laboratory temperature, and the analysis result showed that a

minimal mean ratio was observed in Poisson’ ratio data. Fig. 27 shows that the highest reduction is observed in slant shear for the hybrid specimens with as cast interface due to the weakness in bonding at an elevated temperature.

4. Conclusions

This work investigated the behaviour of homogeneous and hybrid SCC mixtures with basalt fibres. The properties of the mixtures were examined under the effect of fibre dosage, high temperature and method of roughening of the interfacial surface of hybrid concrete. The following main conclusions were obtained.

- The fresh state test results showed that SCC mixtures that meet EFNARC specifications could be manufactured with basalt fibres up to 1.0% volume fraction.

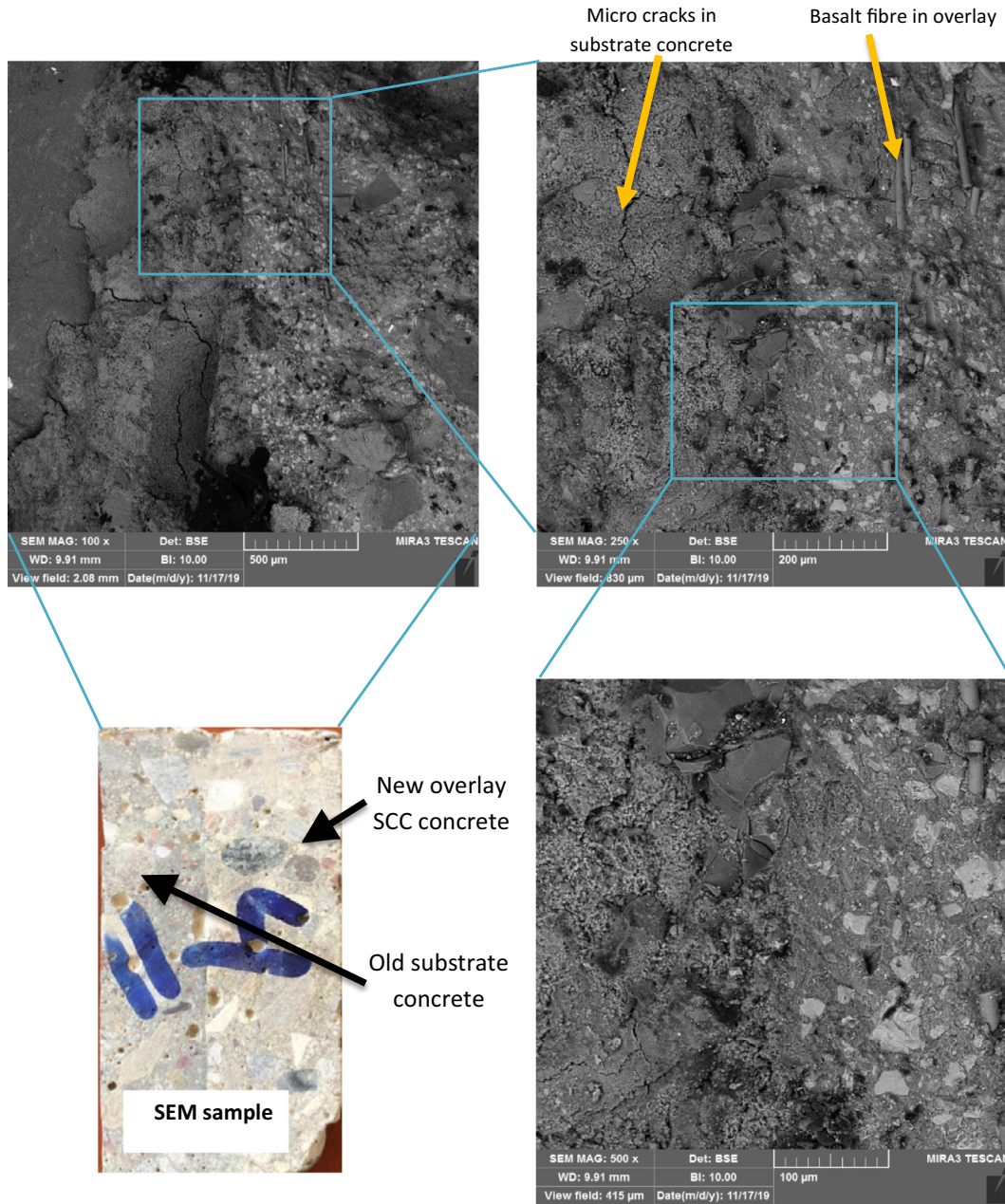


Fig. 25. SEM micrographs of the contact zone between old and new parts of the hybrid concrete sample.

- The compressive strength of the basalt fibre SCC was diminished by 28% when the temperature was increased to 500 °C.
- Increasing the temperature reduced the lateral elongation of the SCC sample and decreased its Poisson's ratio.
- The highest values of elastic modulus for SCC at an elevated temperature of up to 400 °C were obtained by introducing basalt fibres at a dosage of 0.5%.
- The splitting tensile strength of the SCC mixtures was increased by the addition of 0.25% basalt fibre. However, a decrease in splitting tensile strength occurred when more than 0.25% basalt fibre volume fraction was added.
- Considerable degradation was observed in the flexural strength of basalt fibre SCC when the concrete was exposed to a temperature exceeding 300 °C.
- The increment in the basalt fibre dosage of overlay concrete played a remarkable role in improving the slant shear strength of hybrid concrete with a roughened interfacial surface at elevated temperatures.
- Proper bonding between old and new parts of hybrid concrete could be achieved at high temperatures by roughening the interfacial surface through the sandblasting method.

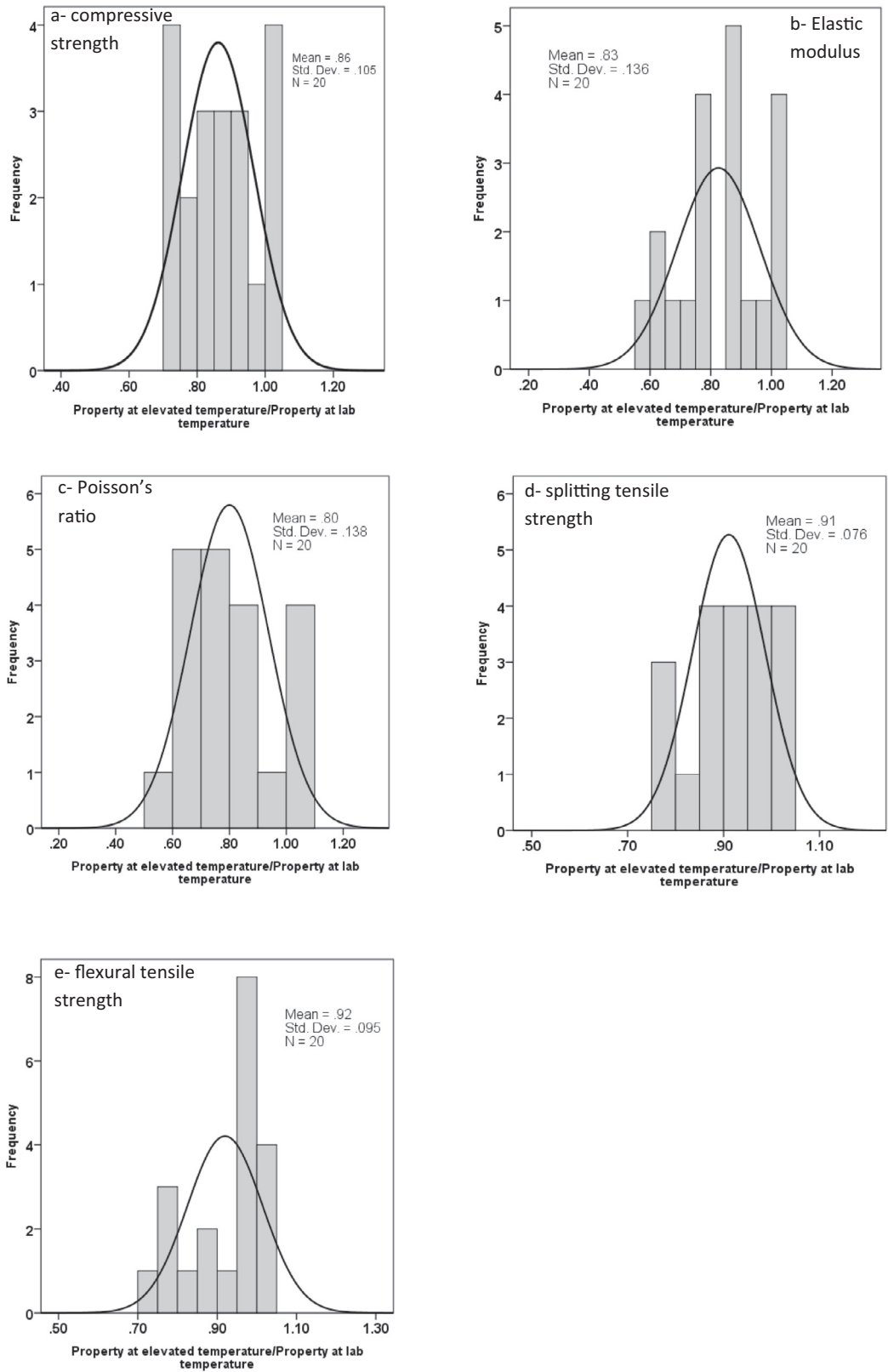


Fig. 26. Histogram for normalized data of the mechanical properties of SCC with respect to the laboratory temperature.

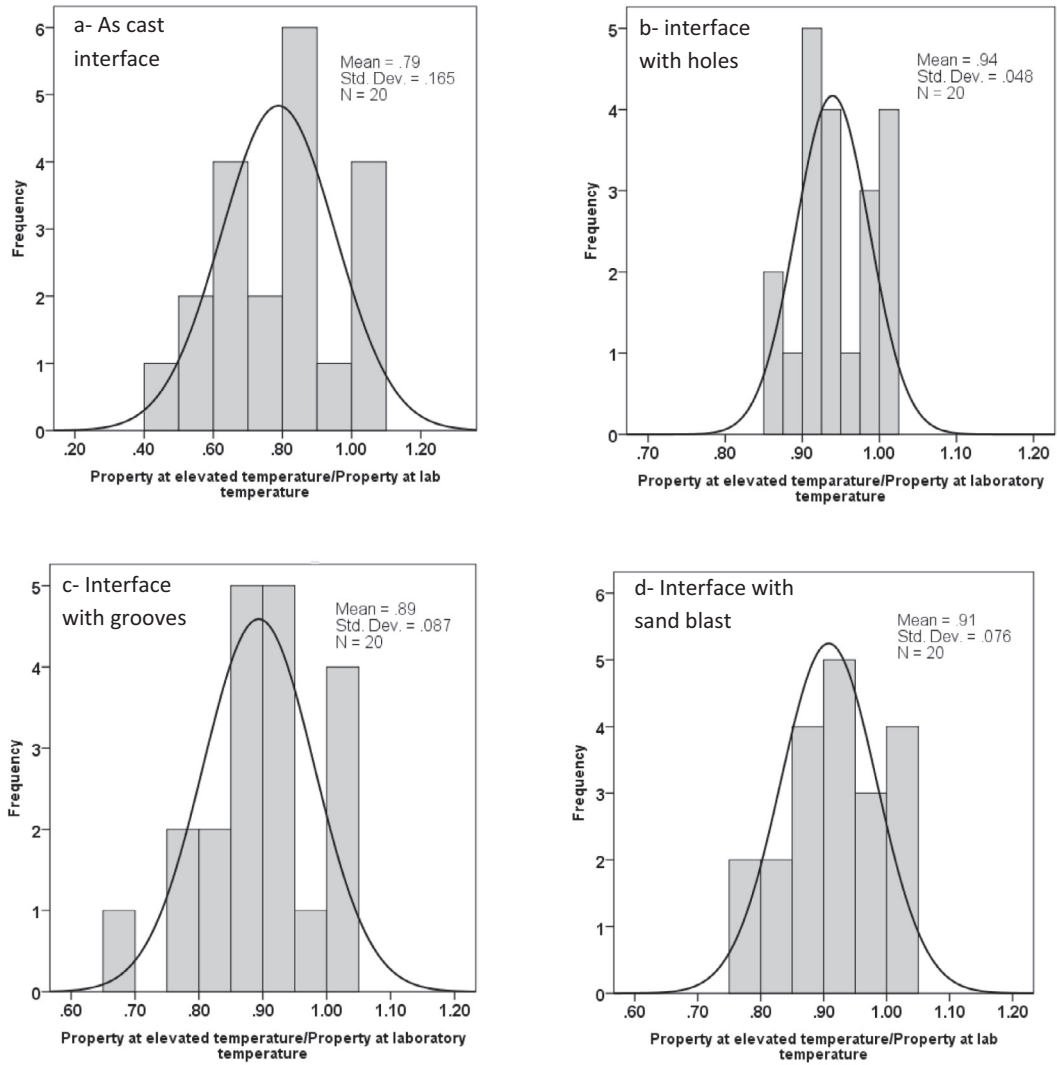


Fig. 27. Histogram for normalized data of the slant shear of hybrid concrete specimens with respect to the laboratory temperature.

Table 6
 Analysis of variance for the mechanical properties of SCCs.

Dependent variable	Independent variable	Sequential sum of squares	Computed F	P value	Significance	Contribution (%)
Compressive strength	BF*	922.24	84.39	0.000	YES	35.61
	T**	1623.99	111.45	0.000	YES	62.70
	Error	43.71	-	-	-	1.69
	Total	2589.95	-	-	-	-
Elastic modulus	BF	28.313	5.29	0.015	YES	6.39
	T	393.318	55.15	0.000	YES	88.78
	Error	21.394	-	-	-	4.83
	Total	443.025	-	-	-	-
Poisson's ratio	BF	0.002175	3.00	0.073	NO	11.18
	T	0.014380	14.88	0.000	YES	73.91
	Error	0.002900	-	-	-	14.91
	Total	0.019455	-	-	-	-
Flexural strength	BF	2.0156	36.11	0.000	YES	13.47
	T	12.7230	170.96	0.000	YES	85.04
	Error	0.2233	-	-	-	1.49
	Total	14.9619	-	-	-	-
Slant shear strength	ST***	4255.52	501.71	0.000	YES	89.18
	BF	23.75	2.80	0.000	YES	0.50
	T	297.26	26.28	0.000	YES	6.23
	Error	195.09	-	-	-	4.09
	Total	4771.61	-	-	-	-

* BF: basalt fibre volume fraction

** T: temperature level

*** ST: interfacial surface roughening method

CRediT authorship contribution statement

James H. Haido: Conceptualization, Supervision, Writing - review & editing. **Bassam A. Tayeh:** Writing - original draft, Writing - review & editing. **Samadar Salim Majeed:** Data curation, Formal analysis, Investigation, Visualization. **Mehmet Karpuzcu:** Conceptualization, Supervision.

Declaration of Competing Interest

The authors declare that they have no known competing financial interests or personal relationships that could have appeared to influence the work reported in this paper.

References

- [1] J.F. Dong, Q.Y. Wang, Z.W. Guan, Material properties of basalt fibre reinforced concrete made with recycled earthquake waste, *Constr. Build. Mater.* 130 (2017) 241–251.
- [2] S.T. Tassew, A.S. Lubell, Mechanical properties of glass fiber reinforced ceramic concrete, *Constr. Build. Mater.* 51 (2014) 215–224.
- [3] F.U.A. Shaikh, Review of mechanical properties of short fibre reinforced geopolymer composites, *Constr. Build. Mater.* 43 (2013) 37–49.
- [4] A.M. Zeyad, A.H. Khan, B.A. Tayeh, Durability and strength characteristics of high-strength concrete incorporated with volcanic pumice powder and polypropylene fibers, *J. Mater. Res. Technol.* 9 (2020) 806–818.
- [5] D.J. Hannant, Fibre reinforced concrete, in: J. Newman, B.S. Choo (Eds.), *Advanced Concrete Technology-processes*, An Imprint of Elsevier, Oxford, 2003, pp. 146–163.
- [6] A.B. Kizilkanat, N. Kabay, V. Akyüncü, S. Chowdhury, A.H. Akça, Mechanical properties and fracture behavior of basalt and glass fiber reinforced concrete: An experimental study, *Constr. Build. Mater.* 100 (2015) 218–224.
- [7] M.M. Kamal, M.A. Safan, Z.A. Etman, B.M. Kasem, Mechanical properties of self-compacted fiber concrete mixes, *HBRC Journal* 10 (1) (2014) 25–34.
- [8] B.A. Tayeh, M.A. Abu Maraq, M.M. Ziara, Flexural performance of reinforced concrete beams strengthened with self-compacting concrete jacketing and steel welded wire mesh, *Structures* 28 (2020) 2146–2162.
- [9] M.A. Ahmadi, O. Alidoust, I. Sadrinejad, M. Nayeri, Development of mechanical properties of self compacting concrete contain rice husk ash, *World Acad. Sci. Eng. Technol.* 34 (2007) 168–171.
- [10] S. Shahidan, B.A. Tayeh, A.A. Jamaludin, N.A.A.S. Bahari, S.S. Mohd, N. Zuki Ali, F.S. Khalid, Physical and mechanical properties of self-compacting concrete containing superplasticizer and metakaolin, *IOP Conf. Ser.: Mater. Sci. Eng.* 271 (2017) 012004, <https://doi.org/10.1088/1757-899X/271/1/012004>.
- [11] J.M. Khatib, Performance of self-compacting concrete containing fly ash, *Construct. Build. Mater.* 22 (2007) 1–4.
- [12] M. Abed, R. Nemes, B.A. Tayeh, Properties of self-compacting high-strength concrete containing multiple use of recycled aggregate, *Journal of King Saud University-Engineering Sciences*. 32 (2020) 108–114.
- [13] P. Kumar, Self-compacting concrete: methods of testing and design, *J. Inst. Eng. (INDIA)* 86 (2006) 145–150.
- [14] I.S. Agwa, O.M. Omar, B.A. Tayeh, B.A. Abdelsalam, Effects of using rice straw and cotton stalk ashes on the properties of lightweight self-compacting concrete, *Constr. Build. Mater.* 235 (2020) 117541.
- [15] A. Serbescu, M. Guadagnini, K. Pilakoutas, Mechanical Characterization of Basalt FRP Rebars and Long-Term Strength Predictive Model, *J. Compos. Constr.* 19 (2) (2015) 04014037, [https://doi.org/10.1061/\(ASCE\)CC.1943-5614.0000497](https://doi.org/10.1061/(ASCE)CC.1943-5614.0000497).
- [16] D.P. Dias, C. Thaumaturgo, Fracture toughness of geopolymeric concretes reinforced with basalt fibers, *Cem. Concr. Compos.* 27 (1) (2005) 49–54.
- [17] J. Ma, X. Qiu, L. Cheng, Y. Wang, Experimental research on the fundamental mechanical properties of presoaked basalt fiber concrete, in: L. Ye, P. Feng, Q. Yue (Eds.), *Advances in FRP Composites in Civil Engineering*, Springer, Berlin, Heidelberg, 2011, pp. 85–88.
- [18] N. Kabay, Abrasion resistance and fracture energy of concretes with basalt fiber, *Constr. Build. Mater.* 50 (2014) 95–101.
- [19] S.A. Yildizel, B.A. Tayeh, G. Calis, Experimental and modelling study of mixture design optimisation of glass fibre-reinforced concrete with combined utilisation of Taguchi and Extreme Vertices Design Techniques, *J. Mater. Res. Technol.* 9 (2) (2020) 2093–2106.
- [20] X. Hu, T. Shen, The applications of the CBF in war industry and civil fields, *HiTech Fiber Appl.* 30 (6) (2005) 7–13.
- [21] J. S.Sim, C. Park, Characteristics of basalt as a strengthening material. for concrete structure. Department of Civil and Environmental. Engineering, Hanyang University, Sa-1-dong, Ansan, Kyunggi 425-791, south Korea 36(6-7) (2005) 504-512.
- [22] A. Palmieri, S. Matthys, M. Tierens, Basalt fibers: mechanical properties and applications for concrete structures. *Concrete solutions: proceedings of the international conference on Concrete Solutions*. CRC Press/Balkema; 2009. p. 165-9.
- [23] J. Wu, H. Li, G. Xian, Influence of elevated temperature on the mechanical and thermal performance of BFRP rebar. CICE 2010. In: 5th int. Conf. FRP composites in Civil engineering, Beijing: Tsinghua University Press; (2010) 69-72.
- [24] Z. Lu, G. Xian, H. Li, Effects of exposure to elevated temperatures and subsequent immersion in water or alkaline solution on the mechanical properties of pultruded BFRP plates, *Compos Part B*. 77 (2015) 421–430.
- [25] D. Brigante, *New Composite Materials: Selection, Design, and Application*, Publishing, Switzerland, Springer International, 2014.
- [26] B.A. Tayeh, B.A. Bakar, M.M. Johari, S.M. Tayeh, Compressive stress-strain behavior of composite ordinary and reactive powder concrete, *Iranica Journal of Energy and Environment*. 4 (3) (2013) 294–298.
- [27] B.A. Tayeh, B.A. Bakar, M.M. Johari, Y.L. Voo, Evaluation of bond strength between normal concrete substrate and ultra high performance fiber concrete as a repair material, *Procedia Eng.* 54 (2013) 554–563.
- [28] B.A. Tayeh, B.A. Bakar, M.M. Johari, Y.L. Voo, Mechanical and permeability properties of the interface between normal concrete substrate and ultra high performance fiber concrete overlay, *Constr. Build. Mater.* 36 (2012) 538–548.
- [29] B.A. Tayeh, B.A. Bakar, M.M. Johari, Characterization of the interfacial bond between old concrete substrate and ultra high performance fiber concrete repair composite, *Mater. Struct.* 46 (2013) 743–753.
- [30] E. Denarié, E. Brühwiler, Structural rehabilitations with ultra-high performance fibre reinforced concretes, *Aedificatio, Int J Restor Build Monument*, 2006, pp. 453–467.
- [31] D.K. Harris, J. Sarkar, T.M. Ahlborn, Interface bond characterization of ultra-high performance concrete overlays, *Transportation Research Board 90th, Annual Meeting* (2011).
- [32] J. Sarkar, characterization of the bond between ultra-high performance concrete substrates, Master of Science Thesis in Civil Engineering, Michigan Technological University, 2010.
- [33] P.M.D. Santos, E.N.B.S. Júlio, Factors Affecting Bond between New and Old Concrete, *ACI Mater. J.* V. 108, No. 4 (2011).
- [34] W. Li, J. Xu, Mechanical properties of basalt fiber reinforced geopolymeric concrete under impact loading, *Mater. Sci. Eng., A* 505 (1-2) (2009) 178–186.
- [35] F. Bayramov, C. Taşdemir, M.A. Taşdemir, Optimisation of steel fibre reinforced concretes by means of statistical response surface method, *Cem. Concr. Compos.* 26 (6) (2004) 665–675.
- [36] Y. Şahin, F. Köksal, The influences of matrix and steel fibre tensile strengths on the fracture energy of high-strength concrete, *Constr. Build. Mater.* 25 (4) (2011) 1801–1806.
- [37] F. Rezaie, S.M. Farnam, Fracture mechanics analysis of pre-stressed concrete sleepers via investigating crack initiation length, *Eng. Fail. Anal.* 58 (2015) 267–280.
- [38] M.G. Alberti, A. Enfedaque, J.C. Gálvez, Fracture mechanics of polyolefin fibre reinforced concrete: Study of the influence of the concrete properties, casting procedures, the fibre length and specimen size, *Eng. Fract. Mech.* 154 (2016) 225–244.
- [39] J. Michels, R. Christen, D. Waldmann, Experimental and numerical investigation on postcracking behavior of steel fiber reinforced concrete, *Eng. Fract. Mech.* 98 (2013) 326–349.
- [40] ASTM, C127–15, Standard Test Method for Relative Density (Specific Gravity) and Absorption of Coarse Aggregate, ASTM International, West Conshohocken, PA (2015).
- [41] ASTM, C128–15, Standard Test Method for Relative Density (Specific Gravity) and Absorption of Fine Aggregate, ASTM International, West Conshohocken, PA (2015).
- [42] EFNARC (2005) Specification and guidelines for self-compacting concrete, <http://www.efnarc.org>
- [43] ASTM, C1621., C1621M–17., Standard Test Method for Passing Ability of Self-Consolidating Concrete by J-Ring, ASTM International, West Conshohocken, PA, 2017.
- [44] ASTM, C39., C39M–18., Standard Test Method for Compressive Strength of Cylindrical Concrete Specimens, ASTM International, West Conshohocken, PA, 2018.
- [45] ASTM, C469., C469M–14., Standard Test Method for Static Modulus of Elasticity and Poisson's Ratio of Concrete in Compression, ASTM International, West Conshohocken, PA, 2014.
- [46] ASTM, C496., C496M–17., Standard Test Method for Splitting Tensile Strength of Cylindrical Concrete Specimens, ASTM International, West Conshohocken, PA, 2017.
- [47] ASTM, C78., C78M–18., Standard Test Method for Flexural Strength of Concrete (Using Simple Beam with Third-Point Loading), ASTM International, West Conshohocken, PA, 2018.
- [48] TS-EN, 12390–8., Testing Hardened Concrete-Part 8: Depth of Penetration of Water under Pressure, Institute of Turkish Standards, Ankara, Turkey, 2002.
- [49] ASTM, C1202–19., Standard Test Method for Electrical Indication of Concrete's Ability to Resist Chloride Ion Penetration, ASTM International, West Conshohocken, PA, 2019.
- [50] Bassam A. Tayeh, B.H. Abu Bakar, M.A. Megat Johari, A.M. Zeyad, Microstructural analysis of the adhesion mechanism between old concrete substrate and UHPFC, *J. Adhes. Sci. Technol.* 28 (18) (2014) 1846–1864.

- [51] A. Al Hallaq, B.A. Tayeh, S. Shihada, Investigation of the bond strength between existing concrete substrate and UHPC as a repair material. Investigation of the Bond Strength Between Existing Concrete Substrate and UHPC as a Repair Material 6 (3) (2017).
- [52] B.A. Tayeh, B.A. Bakar, M.M. Johari, Mechanical properties of old concrete–UHPC interface, Cape Town, South Africa, 2012.
- [53] ACI 211 (2002) Standard Practice for Selecting Proportions for Normal, Heavyweight, and Mass Concrete, ACI Committee Reports, Guides, Standard Practices, and Commentaries, USA.
- [54] ASTM, C882, C882M–13a, Standard Test Method for Bond Strength of Epoxy-Resin Systems Used with Concrete by Slant Shear, ASTM International, West Conshohocken, PA, 2013.
- [55] B.A. Tayeh, B.A. Bakar, M.M. Johari, A.M. Zeyad, The role of silica fume in the adhesion of concrete restoration systems, Advanced Materials Research (Vol. Trans Tech Publications Ltd. 626 (2013) 265–269.